
# Targeting superoxide dismutase to endothelial caveolae profoundly alleviates inflammation caused by endotoxin

Vladimir V. Shuvaev, Raisa Yu. Kiseleva, Evguenia Arguiri, Carlos H. Villa, Silvia Muro, Melpo Christofidou-Solomidou, Radu V. Stan, Vladimir R. Muzykantov

| | |
|---|---|
| PII: | S0168-3659(17)31095-7 |
| DOI: | doi:10.1016/j.jconrel.2017.12.025 |
| Reference: | COREL 9105 |
| To appear in: | *Journal of Controlled Release* |
| Received date: | 27 October 2017 |
| Revised date: | 16 November 2017 |
| Accepted date: | 21 December 2017 |

Please cite this article as: Vladimir V. Shuvaev, Raisa Yu. Kiseleva, Evguenia Arguiri, Carlos H. Villa, Silvia Muro, Melpo Christofidou-Solomidou, Radu V. Stan, Vladimir R. Muzykantov , Targeting superoxide dismutase to endothelial caveolae profoundly alleviates inflammation caused by endotoxin. The address for the corresponding author was captured as affiliation for all authors. Please check if appropriate. Corel(2017), doi:10.1016/j.jconrel.2017.12.025

# Targeting Superoxide Dismutase to Endothelial Caveolae Profoundly Alleviates Inflammation Caused by Endotoxin

Vladimir V. Shuvaev,[1] Raisa Yu. Kiseleva,[1] Evguenia Arguiri,[2] Carlos H. Villa,[1] Silvia Muro,[3] Melpo Christofidou-Solomidou,[2] Radu V. Stan,[4] and Vladimir R. Muzykantov[1,*]

[1]Department of Pharmacology and Center for Translational Targeted Therapeutics and Nanomedicine of the Institute for Translational Medicine and Therapeutics, University of Pennsylvania, Philadelphia, PA

[2]Department of Medicine, Pulmonary, Allergy and Critical Care Division, University of Pennsylvania, Philadelphia, PA

[3]Fischell Department of Bioengineering, University of Maryland, College Park, MD

[4]Department of Biochemistry and Cell Biology, Geisel School of Medicine at Dartmouth, Lebanon, NH

[*]To whom correspondence should be addressed: Vladimir Muzykantov, Translational Research Center, University of Pennsylvania, 3400 Civic Center Blvd., Bldg 421, TRC 10-125, Philadelphia, PA 19104-5158.

Tel.: +1 (215) 898-9823, Fax: + 1 (215) 573-2236.

E-mail: muzykant@mail.med.upenn.edu

**Abstract**

Inflammatory mediators binding to Toll-Like receptors (TLR) induce an influx of superoxide anion in the ensuing endosomes. In endothelial cells, endosomal surplus of superoxide causes pro-inflammatory activation and TLR4 agonists act preferentially via caveolae-derived endosomes. To test the hypothesis that SOD delivery to caveolae may specifically inhibit this pathological pathway, we conjugated SOD with antibodies (Ab/SOD, size ~10nm) to plasmalemmal vesicle-associated protein (Plvap) that is specifically localized to endothelial caveolae in vivo and compared its effects to non-caveolar target CD31/PECAM-1. Plvap Ab/SOD bound to endothelial cells in culture with much lower efficacy than CD31 Ab/SOD, yet blocked the effects of LPS signaling with higher efficiency than CD31 Ab/SOD. Disruption of cholesterol-rich membrane domains by filipin inhibits Plvap Ab/SOD endocytosis and LPS signaling, implicating the caveolae-dependent pathway(s) in both processes. Both Ab/SOD conjugates targeted to Plvap and CD31 accumulated in the lungs after IV injection in mice, but the former more profoundly inhibited LPS-induced pulmonary inflammation and elevation of plasma level of interferon-beta and -gamma and interleukin-27. Taken together, these results indicate that targeted delivery of SOD to specific cellular compartments may offer effective, mechanistically precise interception of pro-inflammatory signaling mediated by reactive oxygen species.

**Key words**: intracellular delivery; endothelial cells; vascular immunotargeting; plasmalemmal vesicle-associated protein; caveolae.

## Introduction

Caveolae are flask-shape invaginations of the cholesterol-enriched domains in the plasmalemma, decorated on the cytosolic side by caveolin-1 [1-4]. They are abundant in the endothelial cells, among some other cell types [5]. Caveolae give rise to the corresponding endocytic vesicles (outer diameter ~60-80 nm) and play a wide range of transporting and signaling functions [4, 6]. Accordingly, caveolae are important targets for pharmacological interventions.

For example, caveolar endocytosis is implicated in action of pro-inflammatory mediators including cytokines and lipopolysaccharide (LPS) [7, 8]. Binding of these mediators to cognate receptor may lead to endocytosis of ligand-receptor complex concomitant with activation NADPH oxidase (NOX) in the membrane of ensuing endosomes [9, 10]. Superoxide anion fluxed by activated NOX in the endosomal lumen mediates intracellular signaling leading to pro-inflammatory endothelial activation [10, 11]. In theory, this pathological pathway can be effectively inhibited by delivery of appropriate antioxidant such as superoxide dismutase (SOD) in the caveolae.

Targeted drug delivery to caveolae in general is an area of high interest, since it may enable unique pharmacological interventions including the trafficking to cellular organelles other than lysosomes and ability to transcytosis [12-14]. For example, affinity ligands of caveolar determinants gp60 (i.e. albumin), aminopeptidase P and Annexin A1 undergo transcytosis [15-18]. Polyelectrolytes were used to target lipid-rich domains of caveolae [19]. Yet, caveolar drug targeting is still in its infancy. Attempts were made to deliver low molecular weight drugs or imaging agents using caveolae-dependent endocytosis such as induced by folate or LDL receptors [20-22]. To our knowledge, there were no reports on caveolar targeting of therapeutic enzymes. Moreover, this is the first study employing Plasmalemmal vesicle-associated protein (Plvap or PV1) as a target for drug delivery.

Plvap localizes specifically in caveolae [23, 24] and fenestrations [25-27]. It is particularly abundant in the caveolae in the pulmonary microvascular endothelium [28]. In this study, we for the first time exploited targeted delivery of a therapeutic enzyme, superoxide dismutase (SOD), to endothelial caveolae using Plvap as the target determinant in order to suppress LPS-mediated pro-inflammatory response.

## MATERIALS AND METHODS

### Reagents and antibodies

Dimethylformamide (DMFA), dimethyl sulfoxide (DMSO), fetal bovine serum, lipopolysaccharide (LPS) from *E. coli* O55:B5, polyinosinic-polycytidylic acid (poly(I:C)), filipin III from *Streptomyces filipinensis*, wortmannin, and (mono)-dansylcadaverine (MDC) were purchased from Sigma (St. Louis, MO). Cu, Zn-superoxide dismutase (SOD) from bovine liver is from Calbiochem (San Diego, CA), 4-[*N*-maleimidomethyl]cyclohexane-1-carboxylate (SMCC), N-succinimidyl-S-acetylthioacetate (SATA) were from ThermoFisher Scientific (Grand Island, NY). Monoclonal antibody MEC-13.3 towards murine PECAM was from BD Biosciences (San Jose, CA). Rat anti-murine Plvap monoclonal antibody IgG2a clone MECA32-secreting hybridoma was obtained from the Developmental Studies Hybridoma Bank (developed under the auspices of the NICHD and maintained at the University of Iowa, Department of Biology, Iowa City, IA 52242). Cells were grown in PFHM-2 (ThermoFisher Scientific) and antibody to murine Plvap was purified using Protein G-Sepharose 4 Fast flow. Rat IgG2a negative control antibody (clone 2A3) was from EMD Millipore. For Western blot analysis (WB) and immunocytochemistry (ICC) the following antibodies were used: goat polyclonal anti-mouse VCAM and anti-mouse PECAM (Santa-Cruz Biotech., Dallas, TX), anti-beta-actin, conjugated to HRP, rabbit monoclonal anti-caveolin-1 (Abcam, Cambridge, MA). The secondary antibodies, anti-goat-HRP were from Santa-Cruz, whereas chicken anti-rabbit Alexa Fluor 488 labeled, goat anti-rat Alexa Fluor 488 or 594 labeled were from Invitrogen (ThermoFisher Scientific), chicken anti-goat Alexa Fluor 647 labeled were from Life Technologies Molecular Probes (ThermoFisher Scientific).

### Conjugate preparation

Antibodies were conjugated with SOD using amino-chemistry. Protected SH-groups were introduced in the molecule of antibody via primary amines using SATA at a molar ratio antibody:SATA 1:20 at room temperature for 30 min followed by SH-groups de-protecting with 50 mM hydroxylamine for 2 h. Maleimide groups were introduce into SOD molecule using SMCC (SOD:SMCC 1:6 molar ration for 1 h at room temperature). Unreacted compounds were always removed by 7K MWCO Zeba Spin Desalting Columns (Thermo). Conjugation was performed at 1:1 Ab:SOD molar ratio for 1 h on ice. The effective diameter of the obtained conjugates was measured by Dynamic light scattering (DLS) using Zetasizer Nano ZSP (Malvern Instruments Ltd., Malvern, UK). Conjugates were frozen and stored at -80°C before use. For binding and bio-distribution studies SOD was radiolabeled with $Na^{125}I$ (PerkinElmer, Waltham, MA) prior to conjugation in order to trace the delivery of drug molecule rather than antibody. Iodination was performed using Pierce Iodination Beads (Thermo Scientific, Rockford, IL) as recommended by the manufacturer. Radioactivity was measured using Wallac 1470 Wizard™ gamma counter (PerkinElmer).

### Cell culture and treatment

Human umbilical vein endothelial cells (HUVEC; Lonza Walkersville, Walkersville, MD) were maintained in EGM-2 medium (Lonza) additionally supplemented with 10% fetal

bovine serum and antibiotic/antimycotic (Invitrogen) in Falcon tissue culture flasks (BD Biosciences, San Jose, CA) pre-coated with 1% gelatin. Murine immortalized endothelial cells bEnd3 were obtained from ATCC (Manassas, VA) and were grown in DMEM supplemented with 10% fetal bovine serum and antibiotic/antimycotic solution. For cell activation LPS or polyinosine-polycytidylic acid (poly(I:C)) were added to cells in complete medium for 4-5 h. Inhibitors were introduced 30 min prior treatment. The following inhibitors were used: 3 µg/ml filipin (caveolin-dependent endocytosis), 0.5 µM wortmannin (macropinocytosis), 50 µM MDC (clathrin-mediated internalization).

**SDS-polyacrylamide gel electrophoresis and Western blotting**

Cells in 24 well culture dishes (app. 100,000 cells per well) were washed twice with phosphate-buffered saline (PBS) and lysed in 100 µl of sample buffer for sodium dodecyl sulfate polyacrylamide gel electrophoresis. Total cellular proteins were subjected to 4-15 % gradient gel, transferred to PVDF membrane (Millipore). The membrane was blocked with 3% nonfat dry milk in TBS-T (100 mM Tris (pH 7.5), 150 mM NaCl, 0.1 % Tween 20) for 1 h followed by incubations with primary and HRP-conjugated secondary antibodies in the blocking solution. The signal was detected using ECL reagents (GE Healthcare).

**Internalization studies**

For internalization studies bEnd3 cells were grown on 1% gelatin coated glass coverslips, treated with Ab/SOD conjugates, washed three times with PBS, fixed with ice-cold 2% paraformaldehyde for 15 min and incubated with Alexa Fluor 594-labeled goat anti-rat IgG (both MECA32 and MEC13 clones are rat monoclonal antibodies) for 1 h at room temperature. Then cells were washed and permeabilized with 0.2% Triton X-100 for 15 min prior staining with Alexa Fluor 488 goat anti-rat IgG for 1 h at room temperature. Samples were washed and mounted using ProLong Gold antifade reagent with DAPI (Invitrogen). Fluorescence images for internalization studies were acquired using a Nikon Eclipse TE2000-U fluorescence microscope equipped with a Plan Apo ×40/1.0 oil objective (Nikon, Tokyo, Japan). Single-labeled conjugates (appeared as green) were considered as internalized while double-labeled conjugates (appeared as yellow) were considered to be extracellular. Microscope control and image processing were carried out using Image-Pro Plus 4.5.1.27 (Media Cybernetics, Bethesda, MD, USA) as described earlier [29]. Internalization rate was calculated as ratio of double-labeled yellow area to total green labeled area and expressed as % Internalization.

**Co-localization studies**

Cells were grown on 1% gelatin coated glass coverslips. After incubation with Ab/SOD cells were washed, fixed with ice-cold 2% paraformaldehyde for 15 min and permeabilized with 0.2% Triton X-100 for 15 min prior staining with antibodies. Conjugates were stained with Alexa Fluor 594-labeled goat anti-rat IgG. Caveolin-1 was stained first with anti-caveolin-1 rabbit antibodies followed by chicken anti-rabbit Alexa Fluor 488 labeled. Co-localization studies were performed on a confocal laser scanning microscope Leica TCS-SP8 (Leica, Germany) using HC PL APO CS2 63x/1.40 Oil objective and 488/552/638 lasers. Image analysis was performed using Volocity 6.3 Cellular Imaging & Analysis.

**Binding of Ab/SOD to endothelial cells**

For binding studies SOD was labeled with $^{125}$I and SOD was conjugated to antibody. Ab/$^{125}$I-SOD conjugates were incubated with cells at 37°C for 1 h, unbound materials were washed out and cells were lysed with lysis buffer (1% Triton X-100, 1.0 M NaOH). Bound radioactivity was measured using a Wallac 1470 Wizard™ gamma counter (Gaithersburg, MD).

**Biodistribution of Ab/SOD conjugates *in vivo***

Animal experiments were performed according to the protocol approved by the Institutional Animal Care and Use Committee (IACUC) of the University of Pennsylvania. $^{125}$I-radiolabeled Ab/SOD conjugates preparation, detailed biodistribution studies and data analysis are described earlier [30]. Tissue radioactivity was determined using a Wallac 1470 Wizard™ gamma counter. The results were used to calculate four parameters characterizing the total and relative SOD uptake, Ab/SOD conjugate biodistribution, and targeting. The percentage of injected dose per gram of tissue (%ID/g) allows comparison of conjugate targeting to different organs and evaluates tissue selectivity of the conjugate uptake. The ratio between %ID/g of an organ and that of blood represents the localization ratio (LR). This parameter normalizes for possible conjugate differences in the circulating levels. Finally, the immunospecificity index (ISI) was calculated as a ratio of LR of targetable conjugate to that of control (nonimmune) conjugates (i.e. ISI = $LR_{Ab}/LR_{IgG}$). ISI is the most objective parameter that estimates targeting specificity [31].

**Endotoxemia model in mice**

The *in vivo* experiments was performed on 6-8 week old male C57BL/6 mice (20-25 g) and conducted in accordance with the guidelines approved by the Institutional Animal Care and Use Committee at University of Pennsylvania. Ab/SOD conjugates (75 µg) were injected i.v. 15 min prior to LPS (0.8 mg/kg) via tail vein [32]. Five hours after the LPS challenge, the lungs were perfused with PBS and harvested. Lungs were added with 1 ml of PBS supplemented with protease inhibitor cocktail and homogenized with 5 mm stainless steel bead using TissueLyser II (both are from Qiagen, Valencia, CA) during 6 min at 30 Hz. Tissue homogenate was further lysed by addition of 0.5% Triton X-100, 0.5% SDS (final concentrations) followed by incubation on rotating platform for 1 h at +4ºC. Homogenates were sonicated with six 3-s strokes at 30% power using a Sonic Processor FB120 (Fisher) and centrifuged 10 min at 16,000 g. Aliquot of clear supernatant was collected and protein concentration in the samples was measured by the DC Protein Assay (Bio-Rad, Hercules, CA). Samples were subjected on Ready gel 4-15% Tris-HCl (Bio-Rad). VCAM and active expressions were analyzed by Western blot using appropriate antibodies and VCAM level was normalized by actin.

**Cytokine measurements**

Plasma cytokines were measured on a BD Accuri C6 Flow Cytometer (BD Biosciences, San Jose, CA) using the LEGENDplex Mouse Inflammation Panel and LEGENDplex v.7.0 software (BioLegend, San Diego, CA). This panel allows simultaneous

quantification of 13 mouse cytokines, including IL-1α, IL-1β, IL-6, IL-10, IL-12p70, IL-17A, IL-23, IL-27, MCP-1, IFN-β, IFN-γ, TNF-α, and GM-CSF.

**Statistical Analyses**

All values were expressed as means±SEM unless indicated otherwise. For comparison of two groups, statistical significance was estimated by Student's t test, where $P \leq 0.05$ was considered significant.

## RESULTS AND DISCUSSION

Endothelial targeting of drugs holds promise to advance pharmacotherapy of many maladies [33-36]. This approach demonstrated superiority over untargeted drugs in numerous animal studies [15, 37-42]. For example, Ab/SOD targeted to endothelium via CD31/PECAM-1 inhibits oxidative stress and inflammation more effectively than untargeted SOD, IgG/SOD or PEG-SOD [7, 32, 37]. Ab/SOD endocytosis seems to be of critical importance in this anti-inflammatory activity [7, 32], since it grants the enzyme an access to its substrate, superoxide anion generated in endothelial endosomes in response to pro-inflammatory agonists [10, 11]. Of note, different agonists use distinct cognate receptors and endocytic pathways. Caveolae were recently implicated in signaling mediated by LPS and TNF [43, 44]. Here we devise targeting SOD to endothelial caveolae, using Plvap as an anchoring molecule [28, 45].

**Antibody/SOD conjugates (Ab/SOD).** Caveolar targeting of nanoparticles is challenging due to limited access. Outer diameter of caveolae has an average outer diameter of ~70 nm [1], while the stomata opening is about 15-40 nm [46]. Conjugation of caveolar ligands yielding compounds bigger than 50-70 nm obliterates targeting [16, 47].

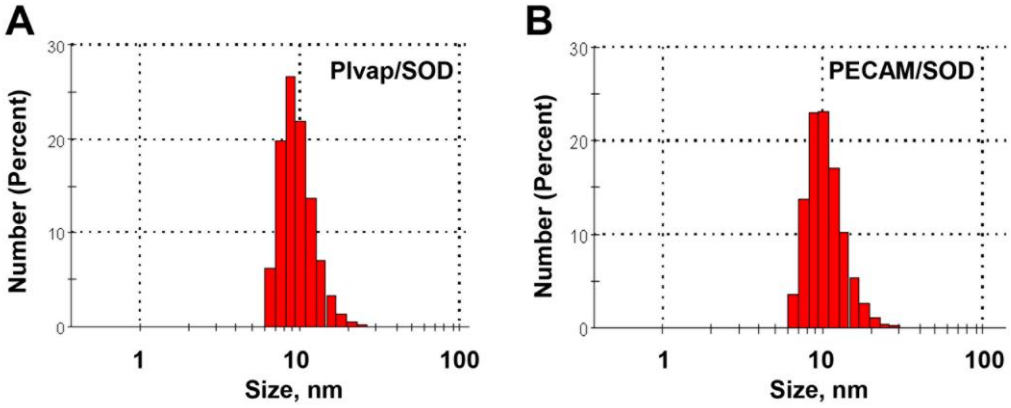


**Figure 1.** DLS analysis of size of Plvap (A) and PECAM Ab/SOD (B). SH-groups were introduced in antibody molecule, while the enzyme was modified to add maleimide group. Conjugation was performed for 1 h at room temperature.

In this study we directly conjugated SOD with rat monoclonal antibodies to Plvap (clone MECA-32), PECAM (clone MEC 13.3) or with negative control rat IgG2a (clone 2A3) using amino-based cross-linking [37]. DLS showed an average size of Ab/SOD close to 10 nm (Fig. 1), with the polydispersity index PDI <0.35. Both relatively modest enlargement of Ab/SOD vs size of unconjugated IgG (~8.5 nm) and results of Western blot analysis (not shown) imply that Ab/SOD are monomolecular conjugates containing one molecule of IgG and SOD each.

**Filipin-sensitive pathway(s) mediate both endothelial activation by LPS and Ab/SOD uptake.** Cellular receptors may serve signaling of inflammatory agonists via specific endosomes [10]. Previous reports implicated TLR4, associated with lipid rafts and caveolae on several cell types, in LPS-mediate signaling, respectively [48-51]. We tested effect of inhibitors of endocytosis on response to LPS in bEnd3 cells,

immortalized murine endothelial cell line [52], that expresses Plvap (Supplement Figure 1).

Filipin, an agent disrupting cholesterol-rich domains of cellular membranes, inhibits endothelial activation by LPS, while macropinocytosis (EIPA) and clathrin-mediated endocytosis (monodansylcadaverine, MDC) inhibitors did not affect it. In contrast, wortmannin, an inhibitor of PI3-kinases, inhibits activation by poly(I:C), a synthetic cognate ligand and agonist of a distinct toll-like receptor TLR3 (Fig.2).

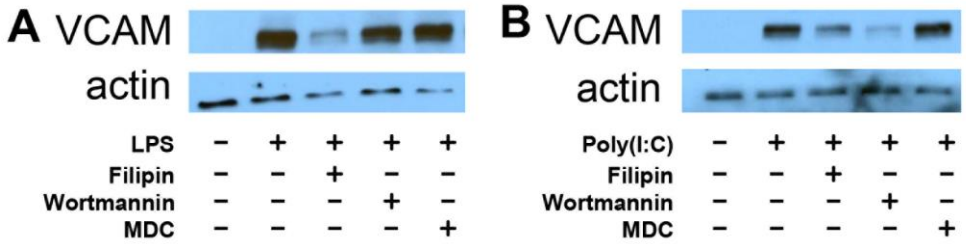


**Figure 2. Effects of endocytosis inhibitors on VCAM expression by HUVEC** in response to LPS (A) and poly(I:C) (B) treatments. Cells were preincubated with filipin (1.5 µg/ml), wortmannin (0.5 µM), or MDC (50 µM) for 30 min followed by 5 h treatment either with LPS (2 µg/ml) or poly(I:C) (200 µg/ml). VCAM expression was probed by Western blotting analysis. Actin was used as gel loading control.

Filipin also inhibited the endothelial endocytosis of Plvap Ab/SOD (Fig.3), thereby implicating cholesterol-rich lipid rafts and caveolae in the uptake of this conjugate. In contrast, filipin did not affect uptake of PECAM Ab/SOD (Fig.3), which squares well with previous reports implicating a non-canonical endocytic pathway distinct from caveolar, clathrin and classical macropinocytosis [53].

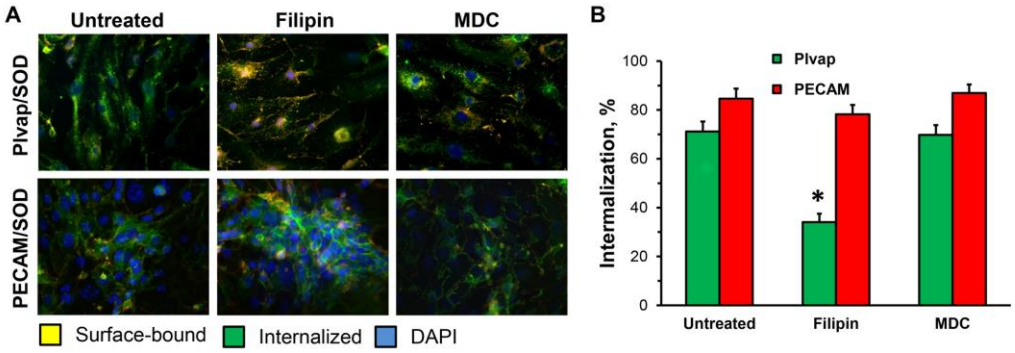


**Figure 3.** Endocytosis of Ab/SOD targeted to Plvap or PECAM by bEnd3 cells treated with 1.5 µg/ml filipin (inhibitor of caveolar endocytosis) or 50 µM monodansylcadaveirine (MDC, inhibitor of clathrin-mediated endocytosis) for 30 min before incubation with Ab/SOD for 1 h. (A). Green and yellow colors are internalized and surface-bound particles, respectively. Nuclei are stained with DAPI (blue). (B). Quantification of the representative images (n≥3; *P≤0.05 treatment vs. untreated control).

Further, Plvap-targeted, but not PECAM-targeted Ab/SOD co-localized with caveolin-1 (Fig. 4). Images analysis showed that Pearson coefficient of co-localization was 0.56±0.07 vs. 0.25±0.08 for Plvap vs. PECAM Ab/SOD, respectively.

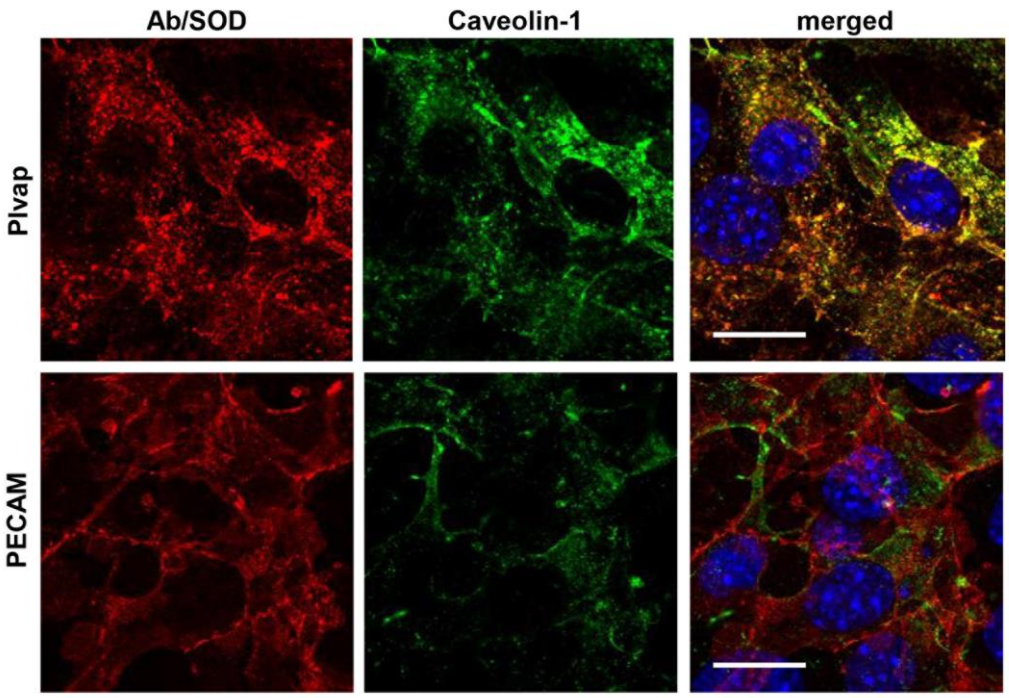


**Figure 4. Co-localization of Ab/SOD conjugates with caveolin-1.** Murine endothelial cells bEnd3 were incubated with Ab/SOD for 2 h on ice to prevent endocytosis, unbound Ab/SOD were washed and cells were exposed for 15 min to 37ºC, then fixed and co-localization of Ab/SOD (red) and caveolin-1 (green) was visualized by confocal microscopy (0.3 µm slice thickness). Nuclei are stained with DAPI (blue). Bar = 20 µm. Representative areas are shown.

Taken together, results presented in this section are consistent with the notion that endothelial cells take Plvap-targeted Ab/SOD via filipin-sensitive endocytic pathway that also serves signaling by LPS. Therefore, Plvap Ab/SOD is targeted to cholesterol-rich endothelial compartments that also can be involved in LPS signaling.

**Binding and effect of Plvap and PECAM Ab/SOD conjugates in bEnd3 cells.** Binding of PECAM Ab/SOD to endothelial cells 30-40-fold exceeded that of Plvap Ab/SOD (Figure 5A). This is not entirely unexpected, because PECAM, commonly used as endothelial cell marker, is expressed at very high level by endothelial cells of any type, whereas Plvap expression is more dependent on the origin and state of the cells and its expression is often significantly reduced or lost in cultured cells.

Nevertheless, bEnd3 cells utilized in this study expressed Plvap at detectable level and responded to LPS by inducible expression of VCAM-1 (Supplement Figures 1 and 2). We used this biomarker as readout of inflammatory endothelial activation in the following studies testing effect of Ab/SOD on LPS-induced endothelial activation.

We found that despite remarkably less effective binding, Plvap Ab/SOD inhibited LPS-induced VCAM-1 expression as effective as highly bound PECAM Ab/SOD (Supplement Figure 3). Based on binding data we calculated efficacy of cell-bound

Plvap and PECAM Ab/SOD and found that the former was an order of magnitude more effective than PECAM-targeted Ab/SOD in inhibition of LPS-induced VCAM response (Fig. 5B).

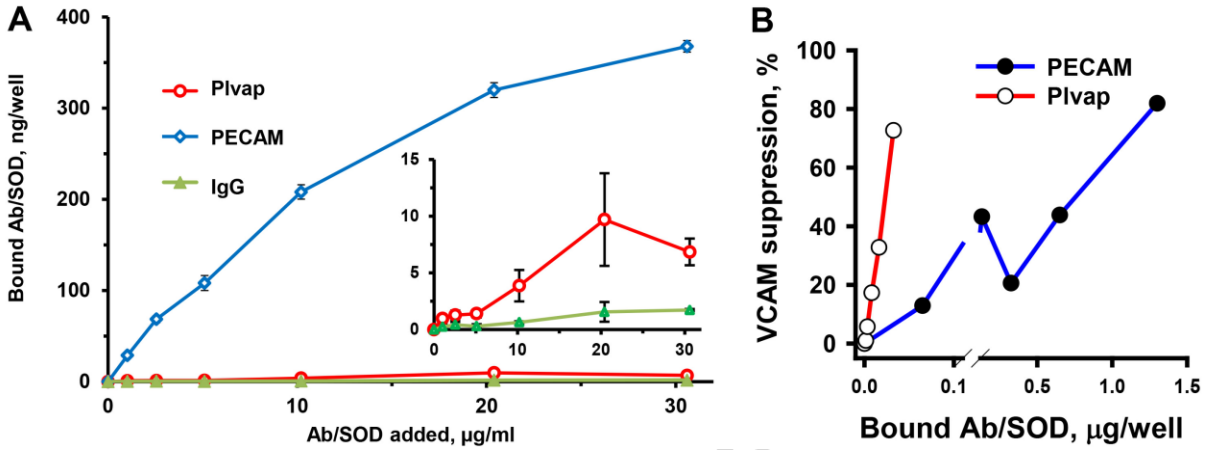


**Figure 5.** Binding of antibody-SOD conjugates to bEnd3 murine endothelial cells and protection against cell activation by LPS. (A). Cells were incubated with Ab/SOD (pre-labeled with $^{125}$I-SOD) for 1 h, washed, and lysed. Bound fraction of labeled SOD was measured using a gamma-counter. Inset, anti-Plvap/SOD binding in zoomed Y axis. (B). Protection of LPS treated cells. Cells were preincubated with incremental concentrations of either anti-Plvap/SOD or anti-PECAM/SOD for 30 min and LPS was added to the medium (2 µg/ml, 5h). Bound fraction was calculated from binding experiments. VCAM expression was detected by Western blotting, quantified, and normalized by actin as gel loading standard.

**Vascular pulmonary targeting and anti-inflammatory effects of Plvap vs. PECAM Ab/SOD.** Cell culture studies have limited relevance to human physiology. For example, immortalized mouse pulmonary endothelial cells internalize Plvap antibody MECA32 via unusual pathway resistant to genetic elimination of caveolin-1, clathrin and dynamin [54]. We embarked on *in vivo* studies in mice as the ultimate validation of trends observed in cell cultures.

To characterize the endothelial targeting we determined accumulation of Ab/SOD in the lungs after intravenous injection in mice. The pulmonary vasculature represents about 20% of the total endothelial surface in the body and receives total cardiac blood output after intravenous (IV) injection, whereas all other organs share the leftovers. For these reasons, agents having endothelial affinity preferentially accumulate in the pulmonary vasculature after IV injection [55].

Tracing of radiolabeled $^{125}$I-SOD conjugated with antibodies to PECAM or Plvap or control IgG showed that 1h after injection the pulmonary uptake of PECAM and Plvap Ab/SOD markedly exceeded that of IgG/SOD (55.3±1.3, 96.2±17.6, and 4.7±0.5 %ID/g of tissue for PECAM, Plvap, and IgG, respectively), while blood level of IgG/SOD was higher than that of PECAM and Plvap Ab/SOD (5.7±1.6, 2.8±0.1, and 17.9±1.6 %ID/g of blood for PECAM, Plvap, and IgG respectively; Supplemental Table S1). Organ-to-blood ratio (i.e. Localization ratio) of PECAM and Plvap Ab/SOD, the parameter of

biodistribution that compensates for differences in the blood pharmacokinetics, was close to 17-20 in lungs for both conjugates (Fig. 6A).

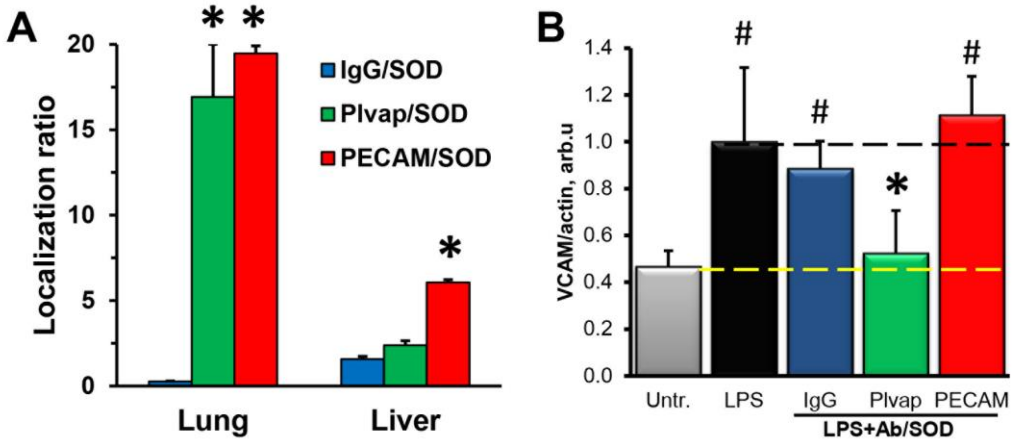


**Figure 6. Biodistribution of Ab/SOD conjugates and protection against LPS. (A)** Pulmonary accumulation of Ab/$^{125}$I-SOD in mice. Shown is Localization ratio, i.e. tissue level as % of injected dose per g of tissue (%ID/g) normalized by %ID/g in blood (*P≤0.05 Ab vs. IgG). (B) Inhibition of LPS-induced VCAM expression in lungs by Ab/SOD, Western blot analysis ($^{\#}$P≤0.05 vs. untreated group, *P≤0.05 vs. LPS-treated group). Data are mean±SEM, n≥3.

To test pro-inflammatory endothelial activation, we determined the level of VCAM-1, the inducible marker of inflammation, in mice challenged with LPS. At the rate-limiting dose at conditions used in the study, PIvap Ab/SOD, but not PECAM Ab/SOD blocked LPS-induced VCAM-1 expression in the lungs (Fig. 6B).

Further we measured the level of circulating cytokines in blood, to evaluate systemic effects of Ab/SOD. PIvap Ab/SOD consistently inhibited LPS-induced elevation of IFNγ, IFNβ and IL-27, whereas PECAM Ab/SOD inhibited the elevation of IFNβ (Fig. 3).

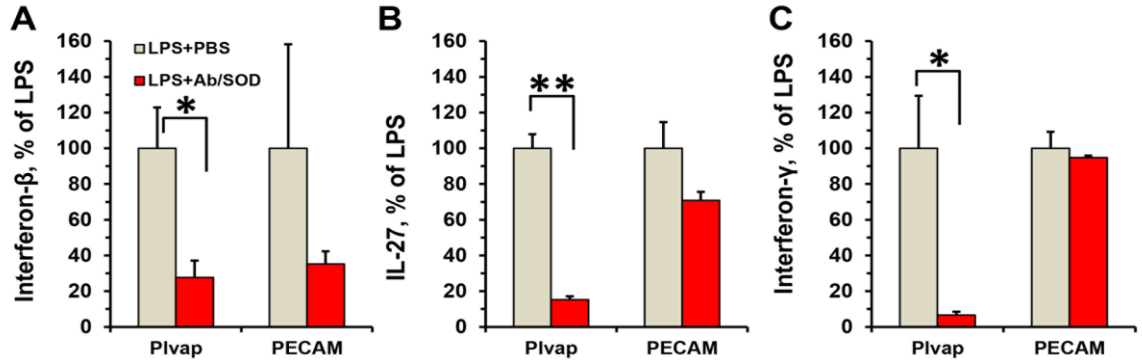


**Figure 7. Protection by PIvap Ab/SOD conjugate against systemic inflammation.** Mice were injected i.v. with Ab/SOD (75 μg) 15 min prior LPS (0.8 μg/kg). After 5 h blood was collected and markers of systemic inflammation interferon-beta (a), interferon-gamma (B) and IL-27 (C) were measured in plasma using flow cytometry. n≥3; *P<0.05, **P<0.001.

IL-27 expression is regulated by NF-κB pathway [56] whereas IFNs are IRF3/NFκB-dependent products [57, 58]. Thus PIvap Ab/SOD presumably inhibits both MyD88- and TRIF-dependent TLR4 signaling.

**LPS does not affect targeting of Plvap Ab/SOD to the pulmonary vasculature**

Based on these results, it is tempting to postulate that by virtue of caveolar targeting Plvap Ab/SOD may provide precise and effective intervention in LPS-mediated vascular inflammation such as in sepsis.

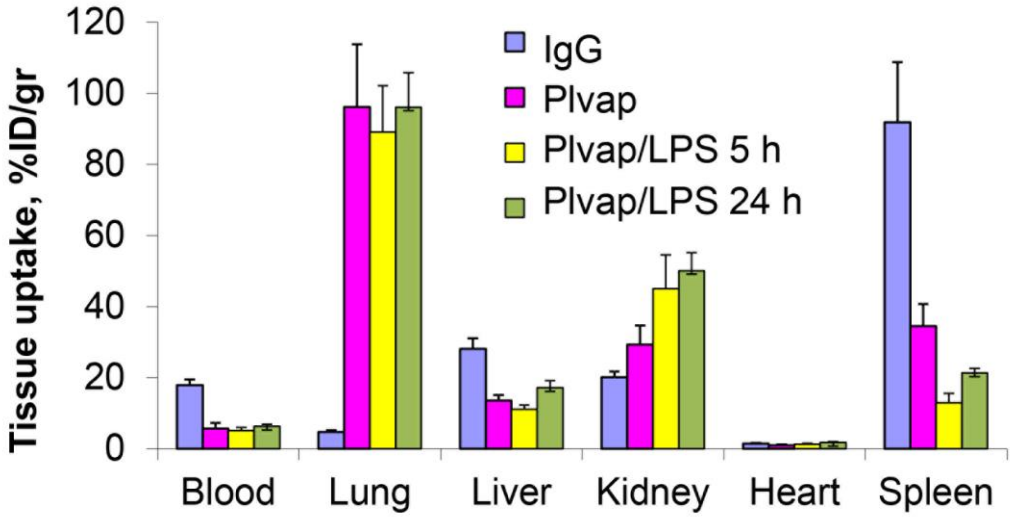


**Figure 8. Effects of LPS on biodistribution of anti-PV1/SOD conjugates.** Animals were treated with LPS (2.0 mg/kg; i.v. injection) for indicated time. with anti-Plvap/$^{125}$I-SOD. Tissues were harvested 1 h post-injection of anti-Plvap/$^{125}$I-SOD and relative loading was measured using gamma-counter. n=3. Note the increase of PV1-dependent targeting in kidney after LPS treatment.

In order to validate this notion, we tested the effect of LPS on targeting of Plvap Ab/SOD in mice. It has been described that LPS may either stimulate endothelial targeting (e.g., directed to ICAM-1) [59], or suppresses it (e.g., directed to ACE) [60, 61]. In contrast, LPS does not affect Plvap-directed pulmonary targeting of Ab/SOD (Figure 8), supporting the notion that this drug delivery approach might be used in the context of inflammation, e.g., for anti-inflammatory therapy.

In summary, results of this study show that caveolar targeting of SOD provides more potent anti-inflammatory effect in animal models of endotoxemia than targeted delivery of SOD to endothelial determinant PECAM, localized in plasmalemma domain(s) distinct from caveolae. This is consistent with the notion that SOD targeted to Plvap gets precisely to endothelial compartment(s) where superoxide anion mediates LPS activation, whereas PECAM-targeted that enters endothelial endosomes via a non-canonical pathway distinct from clathrin and caveolar endocytosis [53].

To our knowledge, this is the first report on targeted delivery of therapeutic enzyme to caveolae. It also shows that this intervention may provide tangible medical benefits. It is tempting to postulate that targeting of SOD to caveolae may boost the efficacy and specificity of blocking pro-inflammatory changes induced by ligands of these cytokines.

We think that superior anti-inflammatory effect of Plvap Ab/SOD vs. PECAM Ab/SOD is attributed to drug addressing to specific endothelial compartments. The latter

binds to endothelial cells abundantly and enters cells via non-canonical endocytosis [12], whereas Plvap Ab/SOD co-localizes with caveolin-1. The exact mechanism of this novel Plvap-dependent endocytic pathway requires further investigation. Plvap is critical for the formation of the stomatal diaphragms of caveolae as well as transendothelial channels and fenestrae [27, 62, 63]. The endothelial diaphragms are important in maintaining permeability of fenestrated vasculature. Without proper diaphragms blood homeostasis became disrupted [27, 64]. Plvap also plays a role in immune response by regulation of leukocytes endothelial transmigration and B cells homeostasis [25, 65]. Thus, more information is necessary to appraise the potential medical utility of Plvap targeting. For example, unanticipated effects on functions of Plvap must be addressed in healthy and pathologically altered animals.

It might seem somewhat counterintuitive that targeting antioxidants requires such a level of precision - not just to cells of interest, or even to the vesicular compartments in these cells, but to the specific type of the vesicles. Reactive oxygen species (ROS) are generally viewed as injurious and/or signaling molecules. ROS have no specific receptors or acceptor molecules. These highly reactive agents act upon variety of biomolecules, hence limited specificity of ROS signaling. However, for the same reason of high reactivity, ROS act in the vicinity of their influx site. The very short distance of ROS action does explain why targeting is needed for their effective and specific interception, especially in vesicular compartments (in contrast to hydrogen peroxide, superoxide anion poorly diffuses via membranes, except via ion channels). Our data reveal a new paradigm of site specific ROS quenching by targeted antioxidant(s). Further investigations are warranted to better understand the mechanisms, opportunities and challenges.

*Acknowledgment.* This work was supported by the National Institutes of Health [Grant RO1 HL073940 ] (to V.R.M.) and ITMAT Pilot Grant (to V.V.S.).

*Supporting Information Available.* Additional Supplemental figures S1, S2 and S3; Supplemental Table S1.

## REFERENCES

[1] R.V. Stan, Structure of caveolae, Biochim Biophys Acta, 1746 (2005) 334-348.
[2] D. Mehta, A.B. Malik, Signaling mechanisms regulating endothelial permeability, Physiol Rev, 86 (2006) 279-367.
[3] J.E. Schnitzer, D.P. McIntosh, A.M. Dvorak, J. Liu, P. Oh, Separation of caveolae from associated microdomains of GPI-anchored proteins, Science, 269 (1995) 1435-1439.
[4] P. Oh, D.P. McIntosh, J.E. Schnitzer, Dynamin at the neck of caveolae mediates their budding to form transport vesicles by GTP-driven fission from the plasma membrane of endothelium, J Cell Biol, 141 (1998) 101-114.
[5] R.G. Parton, M.A. del Pozo, Caveolae as plasma membrane sensors, protectors and organizers, Nat Rev Mol Cell Biol, 14 (2013) 98-112.
[6] E. Shvets, A. Ludwig, B.J. Nichols, News from the caves: update on the structure and function of caveolae, Curr Opin Cell Biol, 29 (2014) 99-106.
[7] V.V. Shuvaev, J. Han, S. Tliba, E. Arguiri, M. Christofidou-Solomidou, S.H. Ramirez, H. Dykstra, Y. Persidsky, D.N. Atochin, P.L. Huang, V.R. Muzykantov, Anti-inflammatory effect of targeted delivery of SOD to endothelium: mechanism, synergism with NO donors and protective effects in vitro and in vivo, PLoS ONE, 8 (2013) e77002.
[8] F.D. Oakley, R.L. Smith, J.F. Engelhardt, Lipid rafts and caveolin-1 coordinate interleukin-1beta (IL-1beta)-dependent activation of NFkappaB by controlling endocytosis of Nox2 and IL-1beta receptor 1 from the plasma membrane, J Biol Chem, 284 (2009) 33255-33264.
[9] S.R. Thomas, P.K. Witting, G.R. Drummond, Redox control of endothelial function and dysfunction: molecular mechanisms and therapeutic opportunities, Antioxid Redox Signal, 10 (2008) 1713-1765.
[10] N.Y. Spencer, J.F. Engelhardt, The basic biology of redoxosomes in cytokine-mediated signal transduction and implications for disease-specific therapies, Biochemistry, 53 (2014) 1551-1564.
[11] M. Ushio-Fukai, Compartmentalization of Redox Signaling through NADPH Oxidase-derived ROS, Antioxid Redox Signal, 11 (2009) 1289-1299.
[12] Z. Wang, C. Tiruppathi, J. Cho, R.D. Minshall, A.B. Malik, Delivery of nanoparticle: complexed drugs across the vascular endothelial barrier via caveolae, IUBMB Life, 63 (2011) 659-667.
[13] M.T. Tarrago-Trani, B. Storrie, Alternate routes for drug delivery to the cell interior: pathways to the Golgi apparatus and endoplasmic reticulum, Adv Drug Deliv Rev, 59 (2007) 782-797.
[14] L. Rajendran, H.J. Knolker, K. Simons, Subcellular targeting strategies for drug design and delivery, Nat Rev Drug Discov, 9 (2010) 29-42.
[15] P. Oh, J.E. Testa, P. Borgstrom, H. Witkiewicz, Y. Li, J.E. Schnitzer, In vivo proteomic imaging analysis of caveolae reveals pumping system to penetrate solid tumors, Nat Med, 20 (2014) 1062-1068.
[16] P. Oh, P. Borgstrom, H. Witkiewicz, Y. Li, B.J. Borgstrom, A. Chrastina, K. Iwata, K.R. Zinn, R. Baldwin, J.E. Testa, J.E. Schnitzer, Live dynamic imaging of caveolae pumping targeted antibody rapidly and specifically across endothelium in the lung, Nat Biotechnol, 25 (2007) 327-337.

[17] D.P. McIntosh, X.Y. Tan, P. Oh, J.E. Schnitzer, Targeting endothelium and its dynamic caveolae for tissue-specific transcytosis in vivo: a pathway to overcome cell barriers to drug and gene delivery, Proc Natl Acad Sci U S A, 99 (2002) 1996-2001.
[18] C. Tiruppathi, W. Song, M. Bergenfeldt, P. Sass, A.B. Malik, Gp60 activation mediates albumin transcytosis in endothelial cells by tyrosine kinase-dependent pathway, J Biol Chem, 272 (1997) 25968-25975.
[19] J. Voigt, J. Christensen, V.P. Shastri, Differential uptake of nanoparticles by endothelial cells through polyelectrolytes with affinity for caveolae, Proc Natl Acad Sci U S A, 111 (2014) 2942-2947.
[20] G. Zheng, J. Chen, H. Li, J.D. Glickson, Rerouting lipoprotein nanoparticles to selected alternate receptors for the targeted delivery of cancer diagnostic and therapeutic agents, Proc Natl Acad Sci U S A, 102 (2005) 17757-17762.
[21] D.S. Theti, V. Bavetsias, L.A. Skelton, J. Titley, D. Gibbs, G. Jansen, A.L. Jackman, Selective delivery of CB300638, a cyclopenta[g]quinazoline-based thymidylate synthase inhibitor into human tumor cell lines overexpressing the alpha-isoform of the folate receptor, Cancer Res, 63 (2003) 3612-3618.
[22] R. Schneider, F. Schmitt, C. Frochot, Y. Fort, N. Lourette, F. Guillemin, J.F. Muller, M. Barberi-Heyob, Design, synthesis, and biological evaluation of folic acid targeted tetraphenylporphyrin as novel photosensitizers for selective photodynamic therapy, Bioorg Med Chem, 13 (2005) 2799-2808.
[23] D. Tse, R.V. Stan, Morphological heterogeneity of endothelium, Semin Thromb Hemost, 36 (2010) 236-245.
[24] R.V. Stan, L. Ghitescu, B.S. Jacobson, G.E. Palade, Isolation, cloning, and localization of rat PV-1, a novel endothelial caveolar protein, J Cell Biol, 145 (1999) 1189-1198.
[25] R. Elgueta, D. Tse, S.J. Deharvengt, M.R. Luciano, C. Carriere, R.J. Noelle, R.V. Stan, Endothelial Plasmalemma Vesicle-Associated Protein Regulates the Homeostasis of Splenic Immature B Cells and B-1 B Cells, J Immunol, 197 (2016) 3970-3981.
[26] R.V. Stan, M. Kubitza, G.E. Palade, PV-1 is a component of the fenestral and stomatal diaphragms in fenestrated endothelia, Proc Natl Acad Sci U S A, 96 (1999) 13203-13207.
[27] R.V. Stan, D. Tse, S.J. Deharvengt, N.C. Smits, Y. Xu, M.R. Luciano, C.L. McGarry, M. Buitendijk, K.V. Nemani, R. Elgueta, T. Kobayashi, S.L. Shipman, K.L. Moodie, C.P. Daghlian, P.A. Ernst, H.K. Lee, A.A. Suriawinata, A.R. Schned, D.S. Longnecker, S.N. Fiering, R.J. Noelle, B. Gimi, N.W. Shworak, C. Carriere, The diaphragms of fenestrated endothelia: gatekeepers of vascular permeability and blood composition, Dev Cell, 23 (2012) 1203-1218.
[28] L.A. Strickland, A.M. Jubb, J.A. Hongo, F. Zhong, J. Burwick, L. Fu, G.D. Frantz, H. Koeppen, Plasmalemmal vesicle-associated protein (PLVAP) is expressed by tumour endothelium and is upregulated by vascular endothelial growth factor-A (VEGF), J Pathol, 206 (2005) 466-475.
[29] R. Wiewrodt, A.P. Thomas, L. Cipelletti, M. Christofidou-Solomidou, D.A. Weitz, S.I. Feinstein, D. Schaffer, S.M. Albelda, M. Koval, V.R. Muzykantov, Size-dependent intracellular immunotargeting of therapeutic cargoes into endothelial cells, Blood, 99 (2002) 912-922.

[30] V.V. Shuvaev, M. Christofidou-Solomidou, F. Bhora, K. Laude, H. Cai, S. Dikalov, E. Arguiri, C.C. Solomides, S.M. Albelda, D.G. Harrison, V.R. Muzykantov, Targeted detoxification of selected reactive oxygen species in the vascular endothelium, J Pharmacol Exp Ther, 331 (2009) 404-411.
[31] A. Scherpereel, J.J. Rome, R. Wiewrodt, S.C. Watkins, D.W. Harshaw, S. Alder, M. Christofidou-Solomidou, E. Haut, J.C. Murciano, M. Nakada, S.M. Albelda, V.R. Muzykantov, Platelet-endothelial cell adhesion molecule-1-directed immunotargeting to cardiopulmonary vasculature, J Pharmacol Exp Ther, 300 (2002) 777-786.
[32] V.V. Shuvaev, J. Han, K.J. Yu, S. Huang, B.J. Hawkins, M. Madesh, M. Nakada, V.R. Muzykantov, PECAM-targeted delivery of SOD inhibits endothelial inflammatory response, FASEB J, 25 (2011) 348-357.
[33] M.D. Howard, E.D. Hood, B. Zern, V.V. Shuvaev, T. Grosser, V.R. Muzykantov, Nanocarriers for vascular delivery of anti-inflammatory agents, Annu Rev Pharmacol Toxicol, 54 (2014) 205-226.
[34] V.V. Shuvaev, V.R. Muzykantov, Targeted modulation of reactive oxygen species in the vascular endothelium, J Control Release, 153 (2011) 56-63.
[35] Z.E. Suntres, Liposomal Antioxidants for Protection against Oxidant-Induced Damage, J Toxicol, 2011 (2011) 152474.
[36] V.V. Shuvaev, J.S. Brenner, V.R. Muzykantov, Targeted endothelial nanomedicine for common acute pathological conditions, J Control Release, 219 (2015) 576-595.
[37] V.V. Shuvaev, S. Muro, E. Arguiri, M. Khoshnejad, S. Tliba, M. Christofidou-Solomidou, V.R. Muzykantov, Size and targeting to PECAM vs ICAM control endothelial delivery, internalization and protective effect of multimolecular SOD conjugates, J Control Release, 234 (2016) 115-123.
[38] E.D. Hood, C.F. Greineder, C. Dodia, J. Han, C. Mesaros, V.V. Shuvaev, I.A. Blair, A.B. Fisher, V.R. Muzykantov, Antioxidant protection by PECAM-targeted delivery of a novel NADPH-oxidase inhibitor to the endothelium in vitro and in vivo, J Control Release, 163 (2012) 161-169.
[39] P.S. Kowalski, P.J. Zwiers, H.W. Morselt, J.M. Kuldo, N.G. Leus, M.H. Ruiters, G. Molema, J.A. Kamps, Anti-VCAM-1 SAINT-O-Somes enable endothelial-specific delivery of siRNA and downregulation of inflammatory genes in activated endothelium in vivo, J Control Release, 176 (2014) 64-75.
[40] K. Nowak, C. Hanusch, K. Nicksch, R.P. Metzger, G. Beck, M.M. Gebhard, P. Hohenberger, S.M. Danilov, Pre-ischaemic conditioning of the pulmonary endothelium by immunotargeting of catalase via angiotensin-converting-enzyme antibodies, Eur J Cardiothorac Surg, 37 (2010) 859-863.
[41] D.A. Dean, Cell-specific targeting strategies for electroporation-mediated gene delivery in cells and animals, J Membr Biol, 246 (2013) 737-744.
[42] H. Li, C.E. Nelson, B.C. Evans, C.L. Duvall, Delivery of intracellular-acting biologics in pro-apoptotic therapies, Curr Pharm Des, 17 (2011) 293-319.
[43] S. Garrean, X.P. Gao, V. Brovkovych, J. Shimizu, Y.Y. Zhao, S.M. Vogel, A.B. Malik, Caveolin-1 regulates NF-kappaB activation and lung inflammatory response to sepsis induced by lipopolysaccharide, J Immunol, 177 (2006) 4853-4860.
[44] M.K. Mirza, J. Yuan, X.P. Gao, S. Garrean, V. Brovkovych, A.B. Malik, C. Tiruppathi, Y.Y. Zhao, Caveolin-1 deficiency dampens Toll-like receptor 4 signaling through eNOS activation, Am J Pathol, 176 (2010) 2344-2351.

[45] R.V. Stan, K.C. Arden, G.E. Palade, cDNA and protein sequence, genomic organization, and analysis of cis regulatory elements of mouse and human PLVAP genes, Genomics, 72 (2001) 304-313.
[46] G.E. Palade, R.R. Bruns, Structural modulations of plasmalemmal vesicles, J Cell Biol, 37 (1968) 633-649.
[47] E.A. Simone, B.J. Zern, A.M. Chacko, J.L. Mikitsh, E.R. Blankemeyer, S. Muro, R.V. Stan, V.R. Muzykantov, Endothelial targeting of polymeric nanoparticles stably labeled with the PET imaging radioisotope iodine-124, Biomaterials, 33 (2012) 5406-5413.
[48] L. Guillot, S. Medjane, K. Le-Barillec, V. Balloy, C. Danel, M. Chignard, M. Si-Tahar, Response of human pulmonary epithelial cells to lipopolysaccharide involves Toll-like receptor 4 (TLR4)-dependent signaling pathways: evidence for an intracellular compartmentalization of TLR4, J Biol Chem, 279 (2004) 2712-2718.
[49] M.W. Hornef, B.H. Normark, A. Vandewalle, S. Normark, Intracellular recognition of lipopolysaccharide by toll-like receptor 4 in intestinal epithelial cells, J Exp Med, 198 (2003) 1225-1235.
[50] M. Pascual-Lucas, S. Fernandez-Lizarbe, J. Montesinos, C. Guerri, LPS or ethanol triggers clathrin- and rafts/caveolae-dependent endocytosis of TLR4 in cortical astrocytes, J Neurochem, 129 (2014) 448-462.
[51] J.S. Pober, W.C. Sessa, Evolving functions of endothelial cells in inflammation, Nat Rev Immunol, 7 (2007) 803-815.
[52] E.F. Wagner, W. Risau, Oncogenes in the study of endothelial cell growth and differentiation, Semin Cancer Biol, 5 (1994) 137-145.
[53] S. Muro, R. Wiewrodt, A. Thomas, L. Koniaris, S.M. Albelda, V.R. Muzykantov, M. Koval, A novel endocytic pathway induced by clustering endothelial ICAM-1 or PECAM-1, J Cell Sci, 116 (2003) 1599-1609.
[54] E. Tkachenko, D. Tse, O. Sideleva, S.J. Deharvengt, M.R. Luciano, Y. Xu, C.L. McGarry, J. Chidlow, P.F. Pilch, W.C. Sessa, D.K. Toomre, R.V. Stan, Caveolae, fenestrae and transendothelial channels retain PV1 on the surface of endothelial cells, PLoS One, 7 (2012) e32655.
[55] V.R. Muzykantov, E.N. Atochina, H. Ischiropoulos, S.M. Danilov, A.B. Fisher, Immunotargeting of antioxidant enzyme to the pulmonary endothelium, Proc Natl Acad Sci U S A, 93 (1996) 5213-5218.
[56] H. Yoshida, C.A. Hunter, The immunobiology of interleukin-27, Annu Rev Immunol, 33 (2015) 417-443.
[57] N.J. Gay, M.F. Symmons, M. Gangloff, C.E. Bryant, Assembly and localization of Toll-like receptor signalling complexes, Nat Rev Immunol, 14 (2014) 546-558.
[58] A.J. Tong, X. Liu, B.J. Thomas, M.M. Lissner, M.R. Baker, M.D. Senagolage, A.L. Allred, G.D. Barish, S.T. Smale, A Stringent Systems Approach Uncovers Gene-Specific Mechanisms Regulating Inflammation, Cell, 165 (2016) 165-179.
[59] H.S. Sakhalkar, M.K. Dalal, A.K. Salem, R. Ansari, J. Fu, M.F. Kiani, D.T. Kurjiaka, J. Hanes, K.M. Shakesheff, D.J. Goetz, Leukocyte-inspired biodegradable particles that selectively and avidly adhere to inflamed endothelium in vitro and in vivo, Proc Natl Acad Sci U S A, 100 (2003) 15895-15900.
[60] W.R. English, P. Corvol, G. Murphy, LPS activates ADAM9 dependent shedding of ACE from endothelial cells, Biochem Biophys Res Commun, 421 (2012) 70-75.

[61] V.R. Muzykantov, E.A. Puchnina, E.N. Atochina, H. Hiemish, M.A. Slinkin, F.E. Meertsuk, S.M. Danilov, Endotoxin reduces specific pulmonary uptake of radiolabeled monoclonal antibody to angiotensin-converting enzyme, J Nucl Med, 32 (1991) 453-460.
[62] L. Herrnberger, K. Ebner, B. Junglas, E.R. Tamm, The role of plasmalemma vesicle-associated protein (PLVAP) in endothelial cells of Schlemm's canal and ocular capillaries, Exp Eye Res, 105 (2012) 27-33.
[63] R.V. Stan, E. Tkachenko, I.R. Niesman, PV1 is a key structural component for the formation of the stomatal and fenestral diaphragms, Mol Biol Cell, 15 (2004) 3615-3630.
[64] A. Elkadri, C. Thoeni, S.J. Deharvengt, R. Murchie, C. Guo, J.D. Stavropoulos, C.R. Marshall, P. Wales, R. Bandsma, E. Cutz, C.M. Roifman, D. Chitayat, Y. Avitzur, R.V. Stan, A.M. Muise, Mutations in Plasmalemma Vesicle Associated Protein Result in Sieving Protein-Losing Enteropathy Characterized by Hypoproteinemia, Hypoalbuminemia, and Hypertriglyceridemia, Cell Mol Gastroenterol Hepatol, 1 (2015) 381-394 e387.
[65] P. Rantakari, K. Auvinen, N. Jappinen, M. Kapraali, J. Valtonen, M. Karikoski, H. Gerke, E.K.I. Iftakhar, J. Keuschnigg, E. Umemoto, K. Tohya, M. Miyasaka, K. Elima, S. Jalkanen, M. Salmi, The endothelial protein PLVAP in lymphatics controls the entry of lymphocytes and antigens into lymph nodes, Nat Immunol, 16 (2015) 386-396.

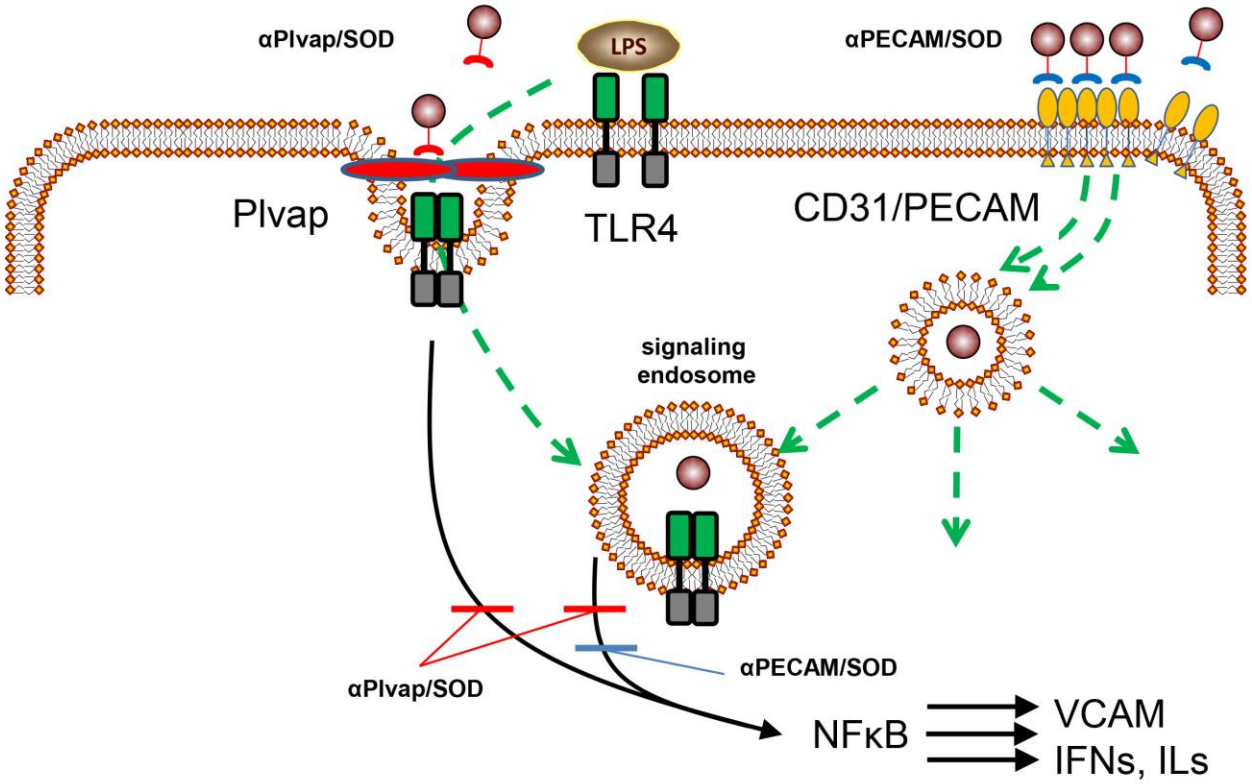


Graphical abstract